

# Conceptual features of improving the flow-through parts of gas separators of submersible electric pumps systems for the production of formation fluid in order to improve the separating properties, energy efficiency and reliability

A Trulev<sup>1</sup>, S Timushev<sup>2</sup> and V Lomakin<sup>3,4</sup>

<sup>1</sup>Rimera Group of companies, Moscow, Russian Federation

<sup>2</sup>Moscow Aviation Institute, Moscow, Russian Federation

<sup>3</sup>Bauman Moscow State Technical University

<sup>4</sup>E-mail: Lomakin@bmstu.ru

**Abstract.** This article analyzes the design of the power part of gas separators of various manufacturers, reveals the causes of backflows, which can lead to hydro-abrasive wear of the elements of the flow-through part, reduction of the separation properties as a result of the gas-liquid mixture flow dispersion, and decrease of pressure gradient in the separation chamber. A mathematical model was selected, hydrodynamic calculations of design options and upgrading were carried out, and an improved flow part of the separator was developed. Bench tests were conducted to confirm the improved parameter of the product.

## Objective

The objective is to analyze the design of the power part of gas separators produced by various manufacturers; to reveal the causes of backflows, which can lead to the reduction of the separation properties as a result of the gas-liquid mixture flow dispersion, and decrease of pressure gradient in the separation chamber; to determine the ways to eliminate relevant hazards; to confirm the effectiveness of the conceptually new design of the gas separator.

The studies were carried out using numerical simulation of the operation of gas separators on water and on gas-liquid mixture. An experimental verification of the numerical calculations was carried out.

## Introduction

At the moment, there is a steady tendency to the increase of depleted wells that currently account for about 30-40% of the total well stock in the Russian Federation. In order to increase the oil recovery rate (ORR), the bottom hole pressure is reduced, respectively, the content of free gas and solids at the pump intake increases.

Works are underway to intensify the flow from the bottom hole zone and increase the oil recovery; hence, some part of the wells is switched to the operating mode with low bottom hole pressures — about of less than 3MPa.

The growth rate of the equipment MTBF (mean time between failures) began to decline, and no it is clear that most of the wells the ESPs with the current wear resistance group can no longer provide a significant increase in the MTBF, since they do not correspond to the changed operating conditions [1].



The serial oilfield submersible pumping equipment is often incapable to operate in such abnormal conditions.

An acute problem is the introduction of an effective technology for their operation with MTBF of at least 600 days [2].

In this regard, the development, study and pilot introduction of innovative technologies for oil production in abnormal conditions with the use of submersible pump systems becomes urgent.

In oil-producing wells with a high gas content, an increase in the efficiency of the electric submersible pumps is achieved by completing them with centrifugal gas separators, in which major portion of free gas separated from the pumped fluid is collected and drawn off to the annular space before the fluid reaches the pump intake.

The efficiency of a centrifugal gas separator significantly depends on the dispersion rate of the gas-liquid structure in the pumped fluid, on the size of gas bubbles, water cut, the presence of surface active agents, the pump intake and discharge pressure [3, 4]. The average diameter of the gas phase bubbles ranges from 40 to 300  $\mu\text{m}$ , for crude oil with high water content — over 130  $\mu\text{m}$  [5]–[11].

In order to increase the efficiency of the oil production process in depleted wells, Rimera Group of Companies has developed and offers a number of new conceptual equipment that is mainly commercialized at present. A conceptual design of pump, pump stages, protectors and gas separators was developed for marginal wells [12]–[20].

The gas separator is considered to be an unreliable element of a pump system due to hydro-abrasive cutting of the body and other elements of the flow-through part. Backflows are formed at the inlet of the axial wheel, auger, provided the pump discharge is more than half the estimated optimal feed [21]. The backflows are a trap for solids — their concentration is rapidly increasing, and the rotating abrasive ring can cut through the body and other elements of the gas separator. [22]–[25].

### Analysis of structural schemes

Fig. 1 shows the design option of a complete gas separator. The following elements are installed in sequence at the intake: auger 4, axial wheel 3, diffuser 2, axial wheel 1.

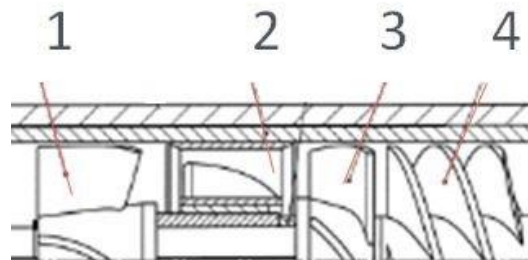


**Fig. 1.** The design option of a complete power part of gas separator.  
Axial wheel 1, diffuser 2, axial wheel 3, auger 4.

An alternating stroke auger can be installed instead of auger 4 and an axial wheel 3.

Analysis of the vortex gas separators of various manufacturers showed that the following structural schemes of the flow part of the gas separator at the intake to the separation chamber are found:

1. Only a fixed stroke auger.
2. An auger and an axial wheel or an alternating stroke auger.
3. A fixed or alternating stroke auger, a diffuser, an axial wheel.
4. An auger, a diffuser of diagonal type, an axial wheel placed inside the cone sleeve, see Fig. 2, [26], [27].

Separation drums with radial fans are installed in the separation chamber of the centrifugal gas separator at the outlet of axial wheel 1. They increase pressure in the peripheral part of the separation chamber, but do not fundamentally change the flow scheme in the vortex separators with axial wheels.

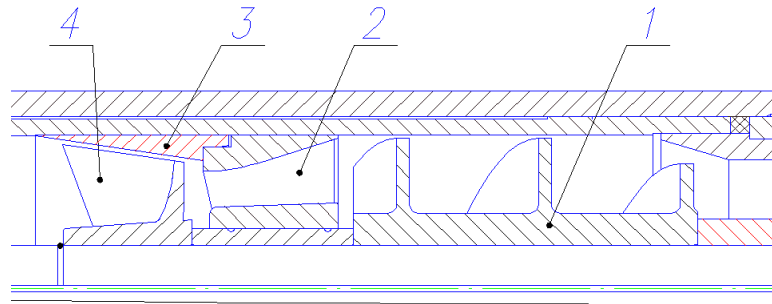


**Fig. 2.** A scheme of the power part of the conceptual design of the gas separator.  
Auger 1, diagonal diffuser 2, Cone sleeve 3, Axial wheel 4.

### Mathematical model

In this article, we use the model of a multiphase incompressible fluid flow ( $\rho = \text{const}$ ). Numerical simulation is based on solving discrete analogs of the basic hydrodynamic equations.

The calculation is carried out on the basis of a mathematical model of a divided multiphase flow. That is, for each phase, the equations of mass and momentum transfer are solved separately, but the pressure field is the same for all phases.

The mathematical model consists of a set of differential and algebraic equations:

1. The volume of the  $i$ -th phase in each calculated cell is calculated as:

$$V_i = \int \alpha_i V dV$$

where  $\alpha_i$  — is the concentration of the  $i$ -th phase in the cell.

The sum of the concentrations of all phases in the cell is one

$$\sum_{i=1}^n \alpha_i = 1$$

2. The equation of conservation of mass (continuity equation):

$$\frac{\partial}{\partial t} \int_V \alpha_i \rho_i dV + \int_A \alpha_i \rho_i \vec{V}_i d\vec{a} = 0$$

where  $\rho_i$  —  $i$ -th phase density

$\vec{V}_i$  —  $i$ -th phase velocity (in the case of turbulent flow modeling by a RANS-type model averaged over time)

3. The equation for the change in the amount of motion:

$$\frac{\partial}{\partial t} \int_V \alpha_i \rho_i dV + \int_A \alpha_i \rho_i (\vec{V}_i \vec{V}_i) d\vec{a} = - \int_V \alpha_i \nabla p dV + \int_V \alpha_i \rho_i \vec{g} dV + \int_A [\alpha_i (T_i + T_i^t)] d\vec{a} + \int_V \vec{M}_i dV$$

where  $(\vec{V}_i \vec{V}_i)$  — tensor product of the velocity vectors of the  $i$ -th phase.

$p$  — pressure

$\vec{g}$  — mass intensity vector (in this case, the gravity force is 9.81 m / s<sup>2</sup> and the inertial force due to the rotation of the computational domain)

$T_i$  — molecular viscosity stress tensor

$T_i^t$  — turbulent stress tensor

$\vec{M}_i$  — vector of total intensity of interfacial interaction forces per unit volume, for a vector  $\vec{M}_i$  fair

equality:  $\sum \vec{M}_i = 0$

Vector  $M_i$  characterizes all the forces that separate phases interact with each other.

$$M_i = \sum_{i \neq j} \left( \overline{F_{ij}^D} + \overline{F_{ij}^{VM}} + \overline{F_{ij}^L} + \overline{F_{ij}^{TD}} + \overline{F_{ij}^{WL}} \right)$$

Where

$\overline{F_{ij}^D}$ — resistance force,  $\overline{F_{ij}^{VM}}$  power of the virtual mass

$\overline{F_{ij}^L}$ — lifting force

$\overline{F_{ij}^{TD}}$ — turbulent dispersion force

$\overline{F_{ij}^{WL}}$ — turbulent dispersion force

### Power of resistance

In the case of modeling the flow of continuous and dispersed media, the resistance force acting on the dispersed medium I from the side of the continuous medium j is equal to:

$$\overline{F_{ij}^D} = A_D \overline{V_r}$$

Where

$A_D$ — linearized drag coefficient

$\overline{V_r} = \overline{V_j} - \overline{V_i}$ — relative velocity of one medium relative to another

$$A_D = C_D \frac{1}{2} \rho_C |\overline{V_r}| \left( \frac{a_{cd}}{4} \right),$$

Where

$C_D$ — drag coefficient

$\rho_C$ — continuous phase density

$a_{cd}$ — interaction area of the phases (in this case, the member  $a_{cd}/4$  is the projected area of the spherical particle on the plane).

The drag coefficient is based on the relation:

$$C_D = f_D C_{D\infty},$$

Where

$C_{D\infty}$ — coefficient of resistance of a single spherical particle moving in an infinite flow

$f_D$ — coefficient taking into account the concentration of particles

$$C_{D\infty} = \frac{24}{Re_d} \left( 1 + 0.15 Re_d^{0.687} \right) n p u Re_d < 1000,$$

and

$$C_{D\infty} = 0.44 n p u Re_d > 1000$$

$$Re_d = \frac{\rho_C |\overline{V_r}| l}{\mu_C}$$

$l$ — characteristic interaction length or bubble size

$\mu_C$ — dynamic viscosity coefficient of continuous medium

Coefficient  $f_D$  is the ratio:

$$f_D = \alpha_C^{nD}$$

$\alpha_C$ — continuous phase concentration

$nD = -8.3$  for spherical particle

## Virtual mass

The inertia of the surrounding fluid affects the acceleration of the particle immersed in the fluid. This effect is modeled by adding mass to the dispersed particle.

The force from the virtual mass acting on phase I, moving rapidly with respect to phase j is found as:

$$\overline{F_{ij}^{VM}} = C_{VM} \rho_C \alpha_C (\overline{a_j} + \overline{a_i})$$

$a_j, i$  — acceleration of jth and ith phase

$C_{VM}=0,5$  — virtual mass coefficient for a spherical particle

## Lift force

In the case where the flow surrounding the dispersed particle is non-uniform or the particle is swirling, it experiences a force perpendicular to the relative velocity.

$$\overline{F_{ij}^L} = C_{Leff} \rho_C \alpha_d (\overline{V_r} \times (\nabla \times \overline{V_c}))$$

$V_r$  — relative phase velocity

$V_c$  — continuous phase speed

$\alpha_d$  — dispersed phase concentration

$C_L=0,25$  — lift force coefficient

## Turbulent dispersion force

Additional change in phase concentrations caused by flow turbulence is modeled as the force of turbulent dispersion

$$\overline{F_{ij}^{TD}} = A_D \overline{V_{TD}}$$

$$F_{ij}^{TD} = A_D V_{TD}$$

$A_D$  — dragforce coefficient

$V_{TD}$  — relative slip speed

$$V_{TD} = D_{TD} (\nabla \alpha_d - \nabla \alpha_c)$$

$D_{TD} = C_0 \nu_t \sigma \alpha I$  — turbulent diffusion tensor

$C_0=1$

$\nu_t$  — turbulent viscosity coefficient kinematic  $\sigma \alpha$  — turbulent Prandtl number

$I$  — unit tensor

$$\sigma \alpha = \sigma_0 \sqrt{1 + C_\beta \xi^2} \frac{1 + \eta}{B + \eta}$$

$$\sigma \alpha = \sigma_0 \sqrt{1 + C_\beta \xi^2} \frac{1 + \eta}{B + \eta}$$

$\sigma_0=1$  — unmodified turbulent Prandtl number

$C_\beta=1,8$  — correction factor

$\xi$  — particle sliding velocity related to the speed of turbulent fluctuations

$\eta$  — particle interaction time related to relaxation time

$b$  — the ratio of the accelerations of the continuous / dispersed phase

$$b = \frac{1 + C_{VM}}{\frac{\rho_d}{\rho_c} + C_{VM}}$$

$$\eta = \frac{\tau_I}{\tau_R}$$

$\tau_I$ — characteristic time of interaction of a particle and a turbulent vortex

$\tau_R$ — particle relaxation time

$$\tau_I = \frac{\tau_T}{\sigma_0} \frac{1}{\sqrt{1 + C_\beta \xi^2}}$$

$$\tau_T = \frac{2}{3} C_\mu \frac{k_c}{\pi \epsilon}$$

$\epsilon$ — continuous phase turbulence energy dissipation rate

$$\tau_R = \tau_D \left( 1 + \frac{\rho_c}{\rho_d} C_{VM} \right)$$

$\tau_D = \frac{\rho_d d^2}{18\mu_c}$ —characteristic time scale for a dispersed particle

$$\xi = \frac{|\overline{V_r}|}{\sqrt{\frac{2}{3} k_c}}$$

$k_c$ — kinetic turbulence energy of the continuous phase

Wall strength

Being located near the solid wall, the gas bubble undergoes an asymmetrical action from the liquid. The force per unit volume that a gas bubble experiences is equal to:

$$\overline{F_{ij}^{VL}} = -C_{WL} \gamma_w \alpha_D \rho_c \frac{|\overline{V_r}|^2}{d_p} \vec{n}$$

Where

$y_w$ — distance from the wall

$\alpha_D$ — dispersed phase concentration

$\rho_c$ — dispersed phase density

$d_p$ — bubble diameter

$C_{WL}$ — coefficient is a function of the distance from the wall and decreasing with increasing distance

$\vec{n}$ — unit normal to the wall at the point closest to the bubble

$V_r, \vec{\tau}$ — tangent to the wall component of the relative velocity

Coefficient  $C_{WL}$  is like:

$$C_{WL} = \max \left( C_{w1} + \left( \frac{C_{w2}}{\gamma_w} \right) d_p, 0 \right)$$

Coefficients are  $C_{W1} = -0,01$ ,  $C_{W2} = 0,05$ .

Thus the force caused by the influence of the wall disappears at a distance from the wall equal to the five diameters of the bubble.

### Mathmodelling results

To carry out hydrodynamic calculations, the geometry of the flow section of the vortex gas separators of various manufacturers was made in accordance with the structural schemes of the Analysis.

Fig.3 shown the places of hydro-abrasive wear of the gas separator body (a), the backflows in the flow part are calculated based on the numerical simulation.

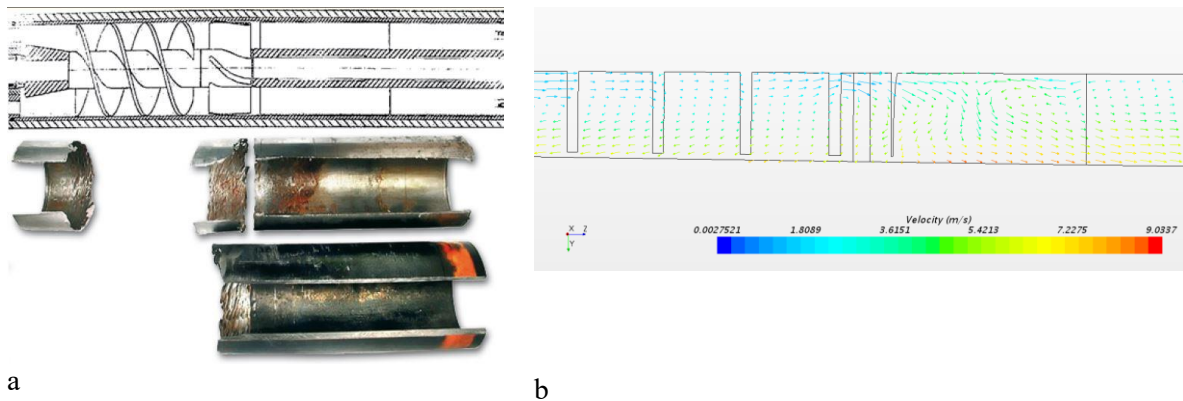


**Fig.3.** The places of hydro-abrasive wear of the gas separator body (a), the backflows in the flow part, obtained by numerical modeling (b).

The auger and the axial wheel have two are as of the rotor with different pressures:

1. The feed auger has about 20 degree inclination angle of the blades at the outlet and, accordingly, a relatively low head.

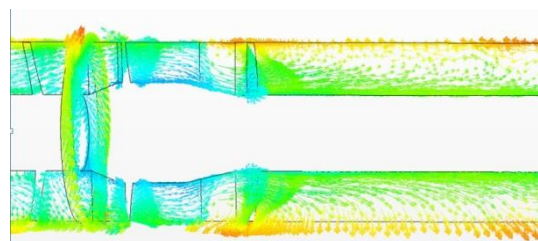
2. The axial wheel has about 90 degree inclination angle of the blades at the outlet and, respectively, a higher head and pressure in the peripheral part.

There are backflows along the peripheral part from the axle wheel back to the auger. Backflows are a trap for solids, the concentration of which increases rapidly, and a rotating abrasive ring of a toroidal vortex can cut through the body due to the hydro-abrasive wear.

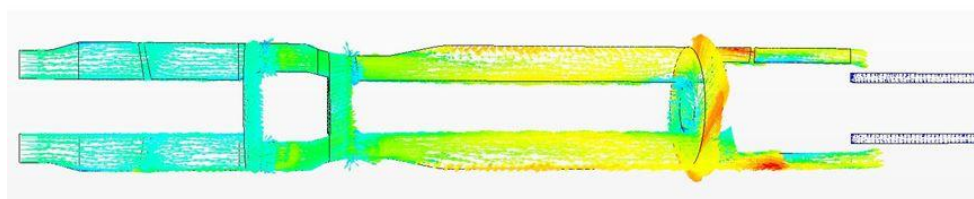
In the case of using an auger of alternating stroke, backflows occur at the modes which are twice or more times lower than the optimal mode, since at large angles of attack the pressure at the inlet decreases.

In the case of using a screw and an axial wheel, backflows can occur in all operating modes.

Fig. 4 shows the velocity plots in the designs of gas separators, the power part of which includes: a fixed stroke an auger, a diffuser, and an axial wheel. In Fig. 4a, the gas separator has an axial diffuser, and in Fig. 4b –a diagonal one with a conical sleeve, inside of which an axial wheel is installed.



a



b

**Fig.4.** Velocity Plots in the design without cone sleeve (a) and with cone sleeve (b).

The cone sleeve separates the low-pressure auger and the high-pressure separation wheel, thus backflows and wear of the sleeve and auger are eliminated.

An analysis of the numerical calculation on water shows that in the design without a cone sleeve, backflows are clearly visible along the periphery from the separation chamber to the inlet of the diffuser. The backflows can lead to hydro-abrasive wear and cutting of the elements of the flow part, the diffuser grid and the housing, to a decrease in the separation properties due to dispersion of the gas-liquid mixture flow and a decrease in the pressure gradient in the separation chamber.

Installing a cone sleeve eliminates, or at least significantly reduces the backflows.

A separation process takes place in the separation chamber a rotating wheel is formed with a partially separated liquid on the periphery. Previously, this wheel pressed on the blades of a stage supplying a gas-liquid mixture, which led to backflows and dispersion. Now the wheel is pressing on the fixed axial bearing in the form of a cone sleeve.

Fig. 5 shows pressure plots in the above designs of gas separators. An analysis of the numerical calculation on water shows that in a structure without a cone sleeve has a lower pressure gradient compared to the structure with the sleeve due to the backflows. The higher is the radial pressure gradient, the more efficient is the separation of free gas from the gas-liquid mixture pumped into the annulus.

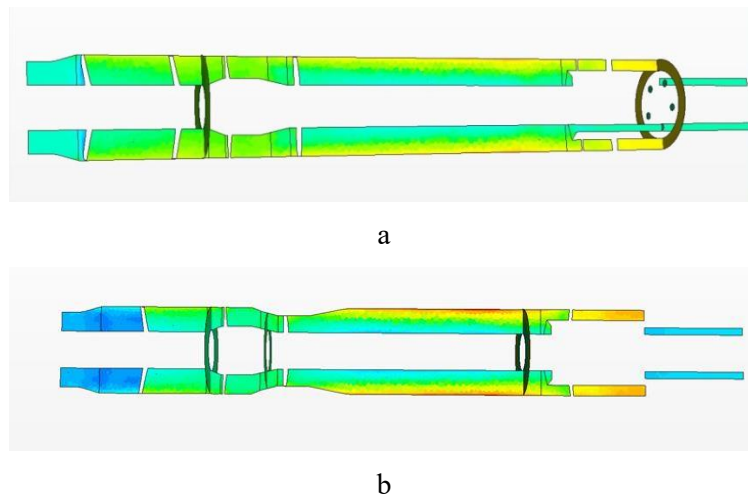


**Fig.5.** Pressure Plots in the design without cone sleeve (a) and with cone sleeve (b).

Fig. 6 shows the results of the calculation of a gas separator with a cone sleeve are presented for gas-liquid mixture.

An analysis of the numerical calculation for the gas-liquid mixture shows that in the separation chamber the process of separation of liquid and free gas occurs. A rotating wheel with a partially separated liquid is formed on the periphery. Previously, this wheel pressed on the blades of a stage supplying a gas-liquid mixture, which led to the backflows, which, in turn, dispersed the gas-liquid mixture, and reduced the pressure in the separation chamber. Now the rotating wheel presses on the fixed axial bearing in the form of a cone sleeve.

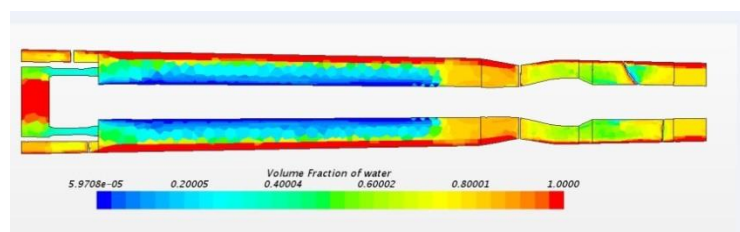


**Fig.6.** Volume fraction of water Plots in the design without cone sleeve

The new conceptual design of submersible gas separators (see Fig. 2) includes the structural separation by a cone sleeve of two areas: the area of delivery of the gas-liquid mixture to the separation chamber and the area of the separation chamber. The axial wheel (auger) delivering the gas-liquid mixture works with maximum feed and minimum pressure, the flow part of the separation area - with maximum head, providing the maximum pressure gradient.

It is necessary to maintain a certain ratio of pressure and feed in the auger. This is due to the fact that gas bubbles can pass through the flow part of the auger without significant separation and the formation of gas locks, which can lead to the delivery failure only at a certain ratio of the surface friction forces associated with the flow velocity and mass inertia forces associated with the pressure gradient.

Vortex and centrifugal gas separators with replaceable elements of the flow part, replaceable augers have been developed for certain supply ranges together with the specialists of the RGU NG Center for Research and Development of RIMERA Group of Companies. At low flow rate, it is proposed to install the augers obtained by reducing the diameter of the serial screws, by cutting, while maintaining the optimal input angles and the range of components.

One of the obvious advantages of gas separators with replaceable augers at the inlet for low rate systems include less power - this saves energy.

For the calculation, the StarCCM software package was used. As the surface mesh, the previously constructed geometry of the flow part was imported.

The following parameters are used as a physical model:

- Multiphase interaction, scale of interaction length 0.1 mm.
- Water H<sub>2</sub>O and gas Air are taken as phases.
- Initial liquid / gas distribution 1/0
- The inlet is set to stagnation at the inlet with a total pressure of 0 Pa and a liquid / gas ratio of 4/1
- At the exit boundary of the fluid, a negative speed is set at 4.5 m / s.
- Atmospheric pressure is set at the gas outlet boundary.

The following parameters were taken as the studied parameters: head, separation coefficient (water fraction at the separator outlet) and power depending on the flow rate.

### Bench test results

Fig. 7 presents the results of bench tests for gas-liquid mixtures in the laboratory of the RSU NG Department of Technology for the development of oil fields.

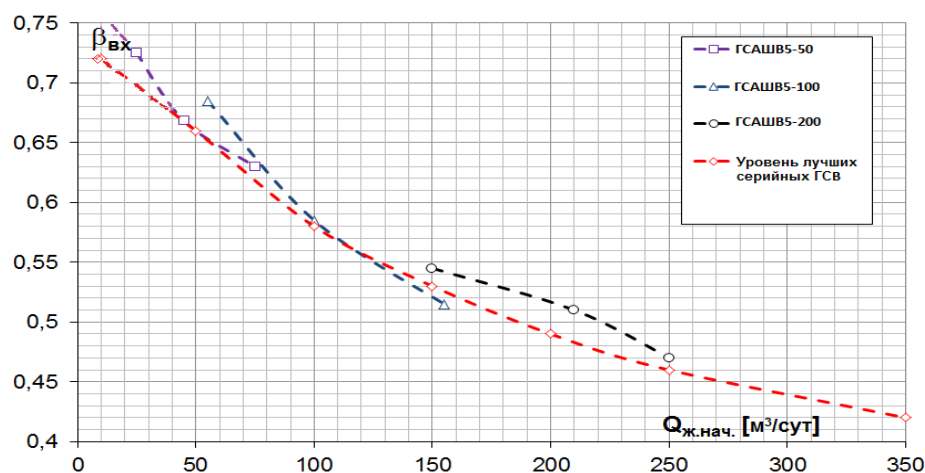


**Fig. 7.** The results of bench tests for gas-liquid mixtures in the laboratory of the RSU NG Department of Technology for the development of oil fields.

Characteristics of a gas separator with replaceable augers for nominal flow rates of 50, 100, 200 cubic meters per day exceed the best serial products [28]–[31].

It is obvious that at low feeds a gas separator with a replaceable screw designed for low flow rate will have less power and higher reliability compared to a conventional gas separator, the power part of which is designed for maximum flow rate.

### Findings

The novelty lies in the fact that the cone sleeve separates two areas: the area of delivery of the gas-liquid mixture to the separation chamber and the area of the separation chamber. The axial wheel (auger) delivering the gas-liquid mixture works with maximum feed and minimum pressure, the flow part of the separation area- with maximum pressure, providing the maximum pressure gradient.

The results of numerical modeling show that:

1. A new conceptual design of gas separators has been developed.
2. Back flows are eliminated or at least significantly reduced in the power elements of the flow part in the new design; such backflows reduce the separation properties and reliability, decrease hydraulic efficiency, and increase power.
3. The results of bench tests for gas-liquid mixtures in the laboratory of the RSU NG Department of Technology for the development of oil fields show, that characteristics of the new gas separator with replaceable augers exceed the best serial products.
4. The conceptual ideas inherent in the design can serve as the basis for the development of the gas separators of other standard sizes.

### List of references:

- [1] Vakhitova R.I., Saracheva D.A., Urazakov D.R., Dumler E.B., Povyshenie effektivnosti raboty pogruzhnykh elektrosentrobeynykh ustanovok pridobycheniya s vysokim gazosoderzhaniem (Improving the efficiency of submersible electric centrifugal plants in oil production with high gas content), Al'met'evsk: Publ. of ASPU, 2019, 104 p.
- [2] Yakimov S.B., Shportko A.A., Shalagin Yu.Yu., Ways of improving gas separators reliability used to protect electric centrifugal pumps (ESP) in the deposits of PJSC "NK "Rosneft" (In Russ.), *Oborudovaniye tekhnologii dlya neftegazovogo kompleksa*, 2017, no. 1, pp. 33–39.
- [3] Yakimov S.B. O vozmozhnosti yakh optimizatsii klassov iznosov ustoychivostiektrosentrobeynykh nasosov name storozhdeniyakh PAO "Orenburgneft": nauch.-tekhn. vestnik. – PAO "NK "Rosneft", 2015. – № 3. – S. 85–92.
- [4] Drozdov A.N., Tekhnologiya i tekhnika dobychi neftipogruzhnyy minasosami v oslozhnennykh usloviyakh (The technology and technique of oil production by submersible pumps in the complicated conditions), Moscow: MAKS press Publ., 2008, 312 p.
- [5] Den'gaev A.V., Povyshenie effektivnosti ekspluatatsii skvazhin pogruzhnykh minasosami pri otkach hkegazozhidkostnykh smesey (Improving the efficiency of well operation by submersible centrifugal pumps during pumping of gas-liquid mixtures): thesis of candidate of technical science, 2005.
- [6] Lomakin V O, Chaburko P S, Kuleshova M S 2017 Multi-criteria Optimization of the Flow of a Centrifugal Pump on Energy and Vibroacoustic Characteristics *Procedia Engineering* **176** pp 476–482
- [7] Lomakin V O, Kuleshova M S, Bozh'eva S M 2016 Numerical Modeling of Liquid Flow in a Pump Station *Power Technology and Engineering* **5** pp 324–327
- [8] Lomakin V O 2015 Proceedings of 2015 International Conference on Fluid Power and Mechatronics
- [9] Lomakin V O, Kuleshova M S, Kraeva E A 2015 Fluid Flow in the Throttle Channel in the Presence of Cavitation *Procedia Engineering* **106** pp 27–35

- [10] Shargatov, V.A., Gorkunov, S.V., Il'ichev, A.T. Dynamics of front-like water evaporation phase transition interfaces (2019) *Communications in Nonlinear Science and Numerical Simulation*, 67, pp. 223–236.
- [11] Arefyev, K.Y., Prokhorov, A.N., Saveliev, A.S. Study of the breakup of liquid droplets in the vortex wake behind pylon at high airspeeds (2018) *Thermophysics and Aeromechanics*, 25 (1), pp. 55–66.
- [12] Trulev A V 2015 New equipment of CJSC Rimera for wells with complicated operating conditions, Proceedings of the conference on mechanized production Oil and Gas Vertical (NeftegazovayaVertikal)19
- [13] Trulev A V 2015 New equipment of OJSC Alnas for wells with complicated operatingconditions *Engineering Practice (Inzhenernayapraktika)* (12) pp 71–73
- [14] Trulev A V, Sabirov A A, Sibirev S V, Verbitsky V S and Timushev S F 2017 Submersible ESP units with wide channels in the flow part for the production of formation fluid from marginal wells with a high content of mechanical impurities *Engineering Practice (Inzhenernayapraktika)* (1–2) pp 60–63
- [15] Trulev A V 2017 Submersible ESP unit of new generation. Innovative solutions for combatting complicated conditions in case of the marginal field, *Oil and Gas Journal Russia* (4) pp 30–34
- [16] Trulev A V 2017 New submersible centrifugal pumps with gray cast iron stages and between bearing design *Engineering Practice (Inzhenernayapraktika)* (5) pp 74–76
- [17] Trulev A V and Grachev V V 2018 Bench tests of a submersible gas and mechanical impurities separator in model mixtures *Gas Industry (Gazovayapromyshlennost')* (8) pp 20–24
- [18] A.V.Trulev, V.F.Loginov, S.I.Gorbunov, S.F.Timushev, A.A.Sabirov, V.O.Lomakin, evelopment and pilot operation of ESP systems of a conceptually new design for the operation of depleted wells with a high content of free gas and mechanical impurities. Composite volume the laureates of the International Competition of Scientific, Technical and Innovative Developments aimed at the development of the fuel and energy and extractive industries in 2019.
- [19] A Trulev, V Verbitsky, S Timushev, P Chaburko Electrical submersible centrifugal pump units of the new generation for the operation of marginal and inactive wells with a high content of free gas and mechanical impurities. *Hydraulics, IOP Conf. Series: Materials Science and Engineering* 492 (2019) 012041 IOP Publishing doi:10.1088/1757-899X/492/1/012041.
- [20] A.V. Trulev, S.F. Timushev. A New Generation of Submersible Electrical Motor Protectors with a Dynamic Labyrinth for Operation in Aggressive Environment with High Concentration of Free Gas and Solids doi: 10.18698/0536-1044-2019-7-59-65.
- [21] Borovskij B.I., Petrov V.I. *Vysokooborotnyelopatochnyenasosy. M., «Mashinostroenie», 1975.*
- [22] Gouskov, A.M., Lomakin, V.O., Banin, E.P., Kuleshova, M.S. Minimization of Hemolysis and Improvement of the Hydrodynamic Efficiency of a Circulatory Support Pump by Optimizing the Pump Flowpath (2017) *Biomedical Engineering*, 51 (4), pp. 229–233. DOI: 10.1007/s10527-017-9720-9
- [23] Arefyev, K.Y., Voronetsky, A.V., Suchkov, S.A., Ilchenko, M.A. Computational and experimental study of the two-phase mixing in gas-dynamic ignition system (2017) *Thermophysics and Aeromechanics*, 24 (2), pp. 225–237. DOI: 10.1134/S086986431702007X
- [24] Lomakin, V.O., Kuleshovav, M.S., Bozh'eva, S.M. Numerical Modeling of Liquid Flow in a Pump Station (2016) *Power Technology and Engineering*, 49 (5), pp. 324–327. DOI: 10.1007/s10749-016-0623-9
- [25] Arefyev, K.Y., Voronetsky, A.V. Modelling of the process of fragmentation and vaporization of non-reacting liquid droplets in high-enthalpy gas flows (2015) *Thermophysics and Aeromechanics*, 22 (5), pp. 585–596.
- [26] A.V.Trulev, G.M. Makrushin, Patent No. 2616331 of the Russian Federation “A method for the efficient operation of submersible blade pumps when pumping off formation fluid with a

- high content of gas and abrasive particles and a gas separator of ESP system for its implementation”. Application date: 31.12.2015.
- [27] A.V.Trulev Patent No. 2503808 of the Russian Federation “Gas separator for a downhole pump”. Application date: 08.07.2011. DOI: 10.1134/S0869864315050078
- [28] Belov, P.A., Kobets, L.P., Borodulin, A.S. Impregnation kinetics of fibers with liquids: Simulation within the generalization of Navier-Stokes equations (2014) *Inorganic Materials: Applied Research*, 5 (4), pp. 403–406.
- [29] Loginov V.F. Kompessionnyenasosydyaneftedobychi v oslozhnennyhusloviyah. // *Oilandgasjournal*. 2016, № 6. C. 54–56.
- [30] D. C. Wilcox (1994). “Turbulence modeling for CFD” // DCW Industries, Inc., 460 pages.
- [31] Aref'Ev, K.Yu., Voronetskii, A.V., Il'Chenko, M.A. Dynamic characteristics of a resonant gas-dynamic system for ignition of a fuel mixture (2013) *Combustion, Explosion and Shock Waves*, 49 (6), pp. 657–661.